Contractile response of alveolar epithelial cells to biochemical or mechanical stimulation probed by traction microscopy

Núria Gavara i Casas

Contractile response of alveolar epithelial cells to biochemical or mechanical stimulation probed by traction microscopy

A dissertation by
Núria Gavara i Casas
in partial fulfilment of the requirements for
the degree of Doctor of Philosophy

Thesis supervisor : Prof. Ramon Farré i Ventura

Unitat de Biofísica i Bioenginyeria
Dept. de Ciències Fisiològiques I
Facultat de Medicina, Universitat de Barcelona.

Chapter 1. Introduction

1.1 The alveolar epithelium

1.1.1 Introduction

To perform their specialized functions most living tissues require a continuous supply of oxygen and a mechanism to remove the carbon-dioxide produced by the metabolism. The lungs provide this function with high efficiency by exchanging oxygen for carbon dioxide between the outside surroundings and the blood. Air flows through the airways by pressure changes produced by lung expansion and relaxation. Inhaled air passes through the nose or mouth, the pharynx, and the larynx (which constitute the upper airway) and through the trachea, bronchi and terminal bronchioles (lower airways), before it reaches the alveoli. The relative thinness (about 0.1 to 0.5 μm) of the alveolar-capillary barrier allows then for easy passive gas exchange by diffusion.

The lung is a dynamic organ that is subjected to mechanical forces throughout development and adult life (Wirtz and Dobbs, 2000). The act of breathing is a mechanical process resulting from the application of cyclical physical stresses at the pleural surface produced by the muscles of the chest wall and the diaphragm (Fredberg and Kamm, 2006). These stresses are then transmitted throughout the lung tissue and the cells adhered to it. In the course of a lifetime, the lung must withstand 10^9 strain cycles with amplitudes that approach 4% during quiet tidal breathing and 10^7 strain cycles with amplitudes that approach 25% during sighs, deep inspirations, or heavy exercise. (Fredberg and Kamm, 2006). In addition, during the process of breathing, the lung tissues are also subjected to

shear due to fluid flow and surface tension at the air-liquid interface (Wirtz and Dobbs, 2000;Waters et al., 2002;D et al., 90 A.D.;Riley et al., 1990).

Besides allowing O_2-CO_2 flux, the lung must also provide the appropriate microenvironment for epithelial cells, endothelial cells, and the other 60 resident cell types in between (Fredberg and Kamm, 2006). In addition, the lungs are also subjected to different physical, chemical, and biological insults. Therefore, they must constitute a viable functional barrier and a meaningful physical deterrent of harmful inhaled microorganisms, allergens, carcinogens, toxic particles, and noxious gases (Maina and West, 2005). The alveolar epithelium is in the front row of the atmosphere-lung interface.

1.1.2 Structure of the alveoli

It is estimated that there are about 300 million alveoli in adult human lungs, each with an average diameter of about 300 μm at 75% maximum lung volume. Alveoli have shared walls through which connective tissue binds adjacent alveoli together (Fig. 1.1). This

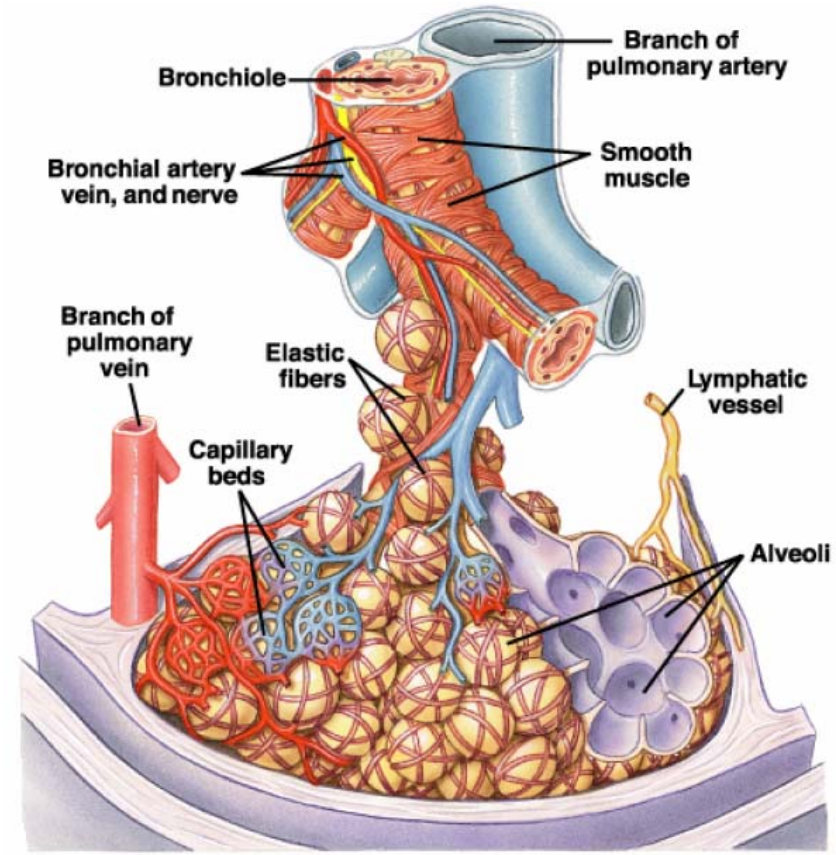

Fig. 1.1 Structure and main components of an alveolar lobule. Adapted from (Silverthorn, 2001).

functional interdependence between neighboring alveoli stabilizes the alveolus and prevents alveolar collapse at low lung volumes (Prange, 2003). The alveoli are almost completely enveloped in pulmonary capillaries (Fig. 1.1). There may be as many as 1000 pulmonary capillaries per alveolus. This results in a vast area of contacts between alveoli and capillaries – probably 50 to 100 m^2 of surface area available for gas exchange by diffusion (Levitzky, 1995;Hlastala and Robertson, 1998). It must be noted that the diffusing capacity for oxygen of a tissue barrier correlates directly with the surface area and inversely with the thickness of the partition (Maina and West, 2005). Accordingly, the alveolar tissue barrier is remarkable for its thinness, thereby allowing for efficient gas exchange.

The alveoli consist of an epithelial layer, an underlying basement membrane and a closely apposed capillary network. Covering the alveolar epithelial layer there is an aqueous surface lining layer containing pulmonary surfactant. The basement membrane (0.15-0.5 μm) is mainly composed of four proteins (collagen IV, laminin, perlecan and entactin), which provide a combination of strength and porosity to the matrix (Maina and West, 2005). Most of the mechanical resistance of the alveolar wall to distention is provided by this basement membrane (Maina and West, 2005). From both the anatomical and the functional point of view, the alveolar blood-gas barrier can be divided into two parts, a thick (supportive) side and a thin (respiratory) side. The thin side (0.2-0.3 μm in thickness, ~50% of the alveolar surface) allows diffusive gas exchange while offering high resistance

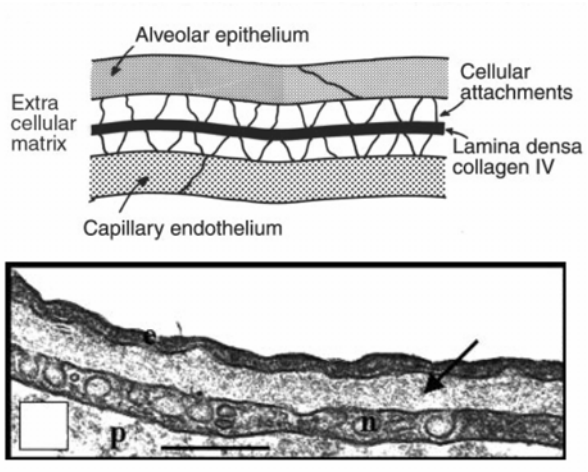

Fig. 1.2 Top: Diagram of the thin side of the blood-gas barrier. Adapted from (West and Mathieu-Costello, 1999). Bottom: Blood-gas barrier of a mammalian lung (Bushbaby, *Galago senegalensis*). **e**, Epithelial cell; **arrow**, extracellular matrix; **n**, endothelial cell; **p**, plasma layer. Scale bars is 3 μm; Adapted from (Maina and West, 2005)

to fluid transport from the capillary to the alveolar space (Fig. 1.2). The thick side (>1 μm in thickness, ~50% of the alveolar surface) contains connecting tissue elements such as collagen I fibers, elastic tissue and interstitial cells such as fibroblasts and pericytes (West and Mathieu-Costello, 1999). These supporting elements provide structural scaffolding of the lung in the alveolar region. Although some gas exchange may occur across it, the thick side mainly allows fluid exchange across the pulmonary capillary (West and Mathieu-Costello, 1999;Maina and West, 2005).

1.1.3 Models of alveolar epithelial cells

Approximately 99% of the alveolar epithelium is composed of two morphologically and functionally distinct cell types: type I and type II cells. Type I, or squamous pneumocytes, are large thin cells (~50-100 μm diameter, 0.05-0.2 μm height except for the nuclear region and volume of 3000 μm^3) that contain few cytoplasmic organelles (Fig. 1.3A). Since they cover 95% of the alveolar epithelial surface and are extremely thin, type I cells are thought to be the main responsible for the diffusive gas exchange (Crandall and Matthay, 2001). Besides, type I cells have an extremely high water permeability and are capable of transporting ions, suggesting that they may play a role in lung liquid homeostasis (Gonzalez et al., 2005;Matthay and Zimmerman, 2005).

Type II cells compose the remaining 5% of the total alveolar epithelium, being preferentially located in corners of the epithelium. Type II cells are smaller and thicker cuboidal cells (10 μm diameter, 5-10 μm height, 550 μm^3 in volume), with many microvilli on their free surface (Fig. 1.3A and B). They contain many cellular organelles, including a large number of secretory granules called lamellar bodies (Fig. 1.3B). Type II cells have two predominant functions. On the one hand, they synthesize, secrete and recycle surfactant, the lining layer of lipoprotein that keeps a low surface tension at the air-surface interface, thereby preventing alveolar collapse. In addition, these cells are also important for alveolar liquid clearance. On the other hand, type II cells maintain the epithelial cell layer through proliferation and differentiation into type I cells (Gonzalez et al., 2005;Matthay and Zimmerman, 2005).

A third cell type in the alveolar epithelium, alveolar macrophages, lie on the top of the extracellular lining provided by type I cells. The function of these cells is to protect the

respiratory surface by phagocytosing microbes and particulate matter, which they carry out by moving freely over the surface of the alveoli. These cells are so efficient that in disease-free lungs the respiratory surface is practically sterile (Maina and West, 2005).

Since type I epithelial cells cover most of the alveolar surface, they may be a more relevant cell model to perform *in vitro* studies of lung injury (Vlahakis et al., 1999). However, establishment of primary type I epithelial cultures has met with limited success. Isolation and culture of alveolar type I cells is difficult because their cytoplasmic extensions are thin and the intercellular junctions they form are very tight (Crandall and Matthay, 2001). Only recently, improvements in the isolation procedures have enabled studies of fresh type I cells *in vitro* (Chen et al., 2004). As a different approach to study the properties of alveolar epithelial cells, type II cells have been extensively used because they can be readily isolated from the lung and studied *in vitro*. Moreover, when plated and grown on plastic, type II cells differentiate into type I cells *in situ*. These metabolic changes begin within the first 24 h of culture and are progressive over several days in culture. Nevertheless, it remains an unanswered question whether the dedifferentiated type II cell is a good model for native type I cells (Dobbs and Gonzalez, 2002). Interestingly, by manipulating extracellular matrix components, soluble factors (such as growth factors), physical shape, mechanical forces, or

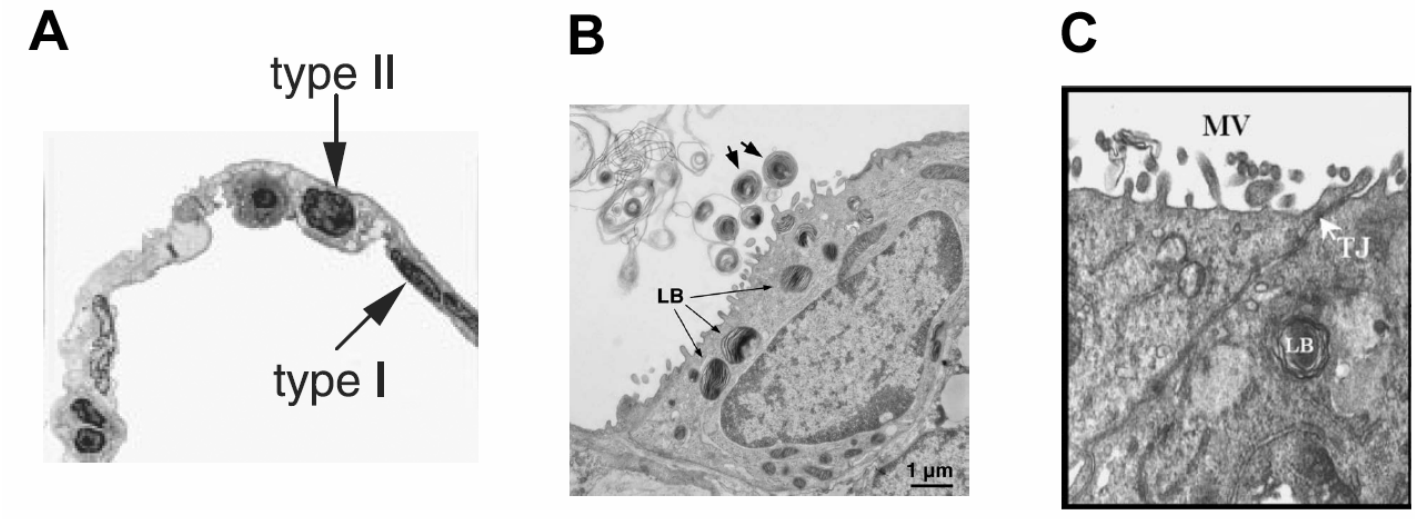

Fig. 1.3 Electron micrographs of alveolar epithelial cells. A: Lung parenchyma showing type I and type II alveolar epithelial cells from a human donor. Adapted from (Fang et al., 2006). B: Rat type II cell. Hallmarks of the typical type II cell morphologic appearance are lamellar bodies (LBs), which contain lipid and protein components. The dense proteinaceous cores of the lamellar bodies can be readily visualized in the secreted LBs (indicated by arrowheads). Adapted from (Dobbs and Gonzalez, 2002) C: Detail of an A549 monolayer grown in a filter. A549 cells exhibit microvilli (MV) on their apical membrane, lamellar bodies (LB), and tight junctions (TJ) between adjacent cells. Original magnification was ×13,000. Adapted from (Lacherade et al., 2001)

the air-liquid interface, cultured alveolar epithelial cells can be induced to retain (or regain) the type II cell phenotype. Two representative cell systems are frequently used as type II models, namely, rat type II epithelial cell cultures at various stages of differentiation (Rannels, 1996;Tschumperlin and Margulies, 1998) and continuous cell lines including A549 (Vlahakis et al., 1999), H441 (Chess et al., 2000), and MLE-12 (Waters et al., 1999).

The studies reported in this thesis were carried out using human A549 cells (Fig. 1.3C). These cells retain a cuboidal shape, express a variety of cytokine and growth factors, exhibit intercellular adhesion molecule-1 surface receptor expression, and possess functioning proinflammatory signaling pathways (Vlahakis et al., 1999). Moreover, unlike primary culture models, they are easy to maintain in culture. Nevertheless, A549 cells have characteristic differences when compared with rat and human alveolar epithelial cells. For instance, in contrast to these primary culture systems, A549 cells secrete less phosphatidyl-glycerol, which is an important component of surfactant active material (Vlahakis et al., 1999). Moreover, they do not form polarized monolayers and probably do not communicate with each other through gap junctions (Stroetz et al., 2001). In this connection, the ability of A549 cells to establish functional tight junctions and to form nonpermeable monolayers has been a matter of controversy. For instance, A549 cells have been suggested to exhibit excessive leakiness to mannitol or dextran (Forbes and Ehrhardt, 2005;Winton et al., 1998). By contrast, A549 cells have been shown to form adherens junctions and tight junctions when grown to confluence (Fig. 1.3C), displaying significant levels of transepithelial electrical resistance (TER) (Kawkitinarong et al., 2004). As regards their response to mechanical and biochemical challenges, A549 cells display similar behavior to that of primary cultures. Vlahakis and coworkers found that after a stretch challenge, A549 cells shared many injury and repair mechanisms with other alveolar epithelial cell lines and primary cell cultures (Vlahakis et al., 2002). Moreover, Umino and coworkers observed that A549 cells and primary rat cells displayed similar contractile behavior after challenge with a contractile agonist (Umino et al., 2000).

1.2 Acute lung injury

Acute respiratory distress syndrome (ARDS) is a common, devastating clinical syndrome of acute lung injury (ALI) that affects both medical and surgical patients. Some

hallmarks of ALI/ARDS are diffuse alveolar damage, presence of neutrophils, macrophages, erythrocytes, hyaline membranes and protein rich edema fluid in the alveolar spaces, capillary injury and disruption of the alveolar epithelium (Mendez and Hubmayr, 2005). Hyaline membranes are homogeneous structures lining along the alveolar septa and containing fibrin as well as cytoplasmic and nuclear debris from sloughed cells (Mendez and Hubmayr, 2005). In histological sections from patients dying of ALI/ARDS, the alveolar epithelium usually exhibits extensive necrosis of alveolar type I cells, leaving a denuded, but mainly intact basement membrane with overlying hyaline membranes (Geiser, 2003).

The loss of epithelial integrity in ALI/ARDS has a number of important consequences. Under normal conditions, the epithelial barrier is much less permeable than the endothelial barrier. Therefore, loss of epithelial integrity will promote alveolar flooding and edema. Furthermore, type II cells provide the major driving force for removal of fluid from the alveolar space by active transport of sodium via ion channels (Matthay and Zimmerman, 2005). As a consequence, loss of type II cells impairs normal epithelial fluid transport, diminishing the removal of edematous fluid from the alveolar space. Finally, injury to type II cells also reduces the production of surfactant, increasing the probability of alveolar collapse when the lung is relaxed.

It is now widely accepted that a variety of triggering disorders can be associated with the development of ALI and injury to the alveolar barrier (Matthay and Zimmerman, 2005). Sepsis is associated with the highest risk of progression to these pathologies. In addition, an intimate relationship between alveolar edema formation and inflammatory and thrombotic effector mechanisms has been recognized. Moreover, it has been suggested that inflammation is a component of many, and perhaps all, causes of direct injury to the alveolar–capillary membrane (Matthay and Zimmerman, 2005). Nevertheless, it is not known how key inflammatory events that are defensive and reparative when they are regulated in lung infection and limited injury become damaging and destructive when they are unregulated in ALI (Matthay and Zimmerman, 2005). On the other hand, it is well established that mechanical ventilation at high volumes can induce or amplify alveolar inflammation and injury and contribute to non-pulmonary organ injury (Matthay and Zimmerman, 2005;Pinhu et al., 2003). This pathological result, thought to be caused by a complex interplay among mechanical forces acting on lung structures during mechanical

ventilation, is named ventilator induced lung injury (VILI). There is increasing evidence that the mechanical forces applied during mechanical ventilation can injure the lung in two inter-related and overlapping ways: through physical disruption of the tissues and cells, and through activation of cytotoxic or proinflammatory responses (Pinhu et al., 2003). Moreover, it should be kept in mind that patients already suffering ALI/ARDS often require high levels of supplementary oxygen and/or mechanical ventilation (Matthay and Zimmerman, 2005). Therefore, this unavoidable clinical practice further extends the interplay between inflammatory and mechanical insults in ALI or VILI.

1.3 Integrity of the alveolar-capillary barrier

The normal functioning of the lungs depends on the establishment and maintenance of a monolayer of epithelial cells separating the airspace and the capillary. The epithelial monolayer acts as a regulated semipermeable barrier that limits the passive diffusion of liquids and solutes but permits gas exchange (Dudek and Garcia, 2001;Fink and Delude, 2005). In addition, this barrier function is also important to prevent systemic contamination by microbes and toxins that are present in the external environment (Fink and Delude, 2005). Therefore, the integrity of the alveolar epithelial monolayer is a critical requirement for preservation of pulmonary function. As it has been described above, loss of epithelial integrity in acute lung injury is characterized by alveolar flooding and edema. Under these pathologic conditions, movement of fluid, macromolecules, and leukocytes into the alveolar air spaces takes place primary by paracellular pathways, as a result of the formation of paracellular gaps in the disrupted epithelial monolayer (Dudek and Garcia, 2001). Such gaps are the result of an unbalance of forces at the cell level.

1.3.1 Force balance in the epithelial monolayer

The epithelial monolayer integrity is believed to be regulated by a balance of competing forces at the sites of cell-cell and cell-matrix attachment (Fig. 1.4) (Dudek and Garcia, 2001). Centripetal tension results from active contractile forces and passive cell stiffness, whereas centrifugal forces result from adhesive cell-cell and cell-matrix tethering

forces. Activation of centripetal tension and/or reduction of centrifugal forces entail the occurrence of gaps between the cells thereby increasing transepithelial permeability. Interestingly, both competing forces in this model are intimately linked to the actin cytoskeleton. Epithelial cells contain an abundance of the molecular machinery necessary to generate tension via actomyosin motors. In addition, in the mechanically dynamic environment of the lungs, cell stiffness passively contributes to centripetal tension due to cytoskeleton recoil (Trepat et al., 2004). The actin cytoskeleton also regulates centrifugal forces by being focally linked to multiple membrane adhesive proteins. Some of them are cadherins, which attach to the actin cytoskeleton via catenins forming adherens junctions; functional intercellular proteins of the zona occludens (ZO) and zona adherens which build up tight junctions; and proteins forming focal adhesion complexes. These adhesive proteins provide the epithelial monolayer with adhesive strength to resist separation of cells from the substratum and adjoining cells through their links with the actin cytoskeleton.

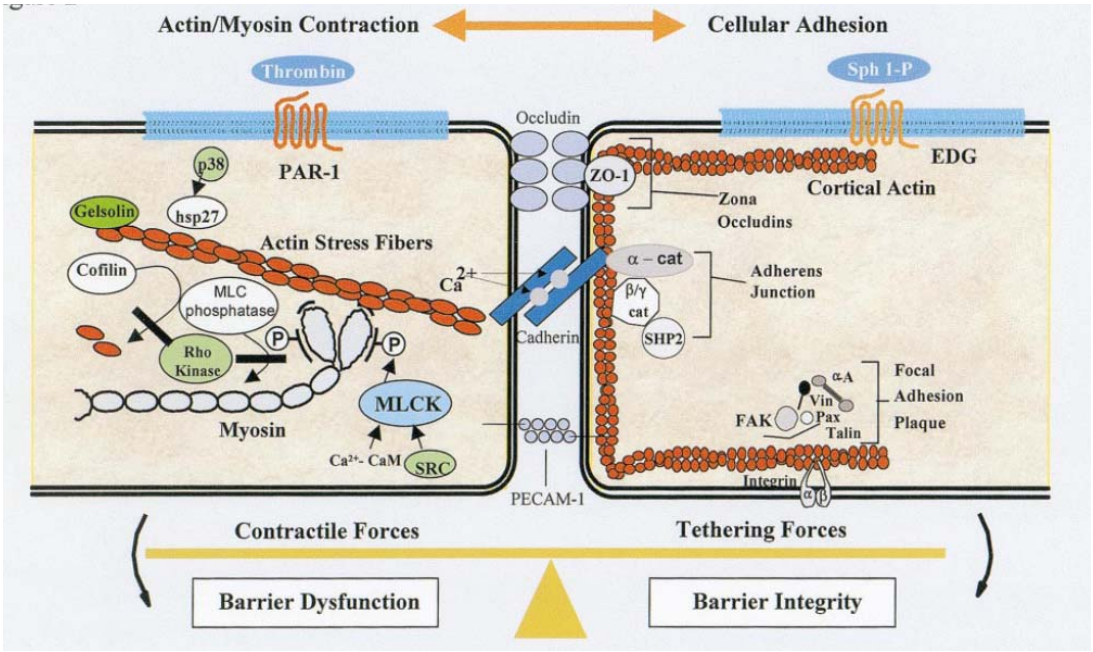

Fig. 1.4. Force balance regulating barrier integrity. Actomyosin contractile elements and cellular adhesive forces regulate paracellular gap formation. When contractile forces predominate, as depicted in the thrombin stimulated model (left), epithelial cells pull apart to form paracellular gaps, favoring barrier disruption. Left side: schematic representation of the major components and pathways involved in regulating actomyosin contraction. Right side: cell-cell and cell-matrix contacts that link epithelial cells into a functional barrier. When these tethering forces predominate, a thick cortical actin ring is observed, whereas epithelial cells maintain tight connections with each other and the underlying matrix to tilt the balance toward increased barrier integrity. Also depicted are proteins involved in tight and adherens junctions and their linkage to the actin cytoskeleton. Adapted from (Dudek and Garcia, 2001)

The presence of inflammatory mediators and/or monolayer distention induced by mechanical ventilation, which are characteristic features of acute lung injury, can affect the mechanical and adhesive properties of alveolar epithelial cells. As a consequence, these stimuli may result in impairment of the barrier integrity and disruption of the epithelial monolayer. Focusing on the centripetal component of the described force balance, the stiffening response of alveolar epithelial cells to biochemical or mechanical stimuli as been extensively studied (Trepat et al., 2004;Trepat et al., 2005;Trepat et al., 2006). These studies showed that stimuli characteristic of ALI result in cell stiffening, thus increasing centripetal tension and impairing the force balance in the epithelial barrier. Nevertheless, studies on the active contractile response of alveolar epithelial cells to these two types of stimuli (inflammation and stretch) are lacking. Knowledge of the contractile properties of alveolar epithelial cells and their behaviour after biochemical or mechanical challenges will help us to further our understanding on the integrity of the epithelial barrier in the pathological conditions that characterize ALI. This thesis contains two studies of the contractile response of alveolar epithelial cells to stimuli characteristic of ALI. On the one hand, thrombin has been used as an inflammatory stimulus. On the other hand, cell stretch induced by substrate deformation has been used to simulate some characteristics of mechanical ventilation.

1.3.2 Thrombin as an inflammatory stimulus inducing contractile response in alveolar epithelial cells.

An extensively-studied model of alveolo-capillary barrier dysfunction is the one evoked by thrombin, a central regulatory protease in the coagulation cascade. Thrombin is an effective inflammatory mediator, acting via multiple mechanisms to initiate an inflammatory response (Moffatt et al., 2004a). Interestingly, most inflammatory lung diseases are characterized by episodic plasma leakage, during which thrombin may leave the circulation (Moffatt et al., 2004b). Moreover, a considerable number of *in vitro* studies have shown that thrombin disrupts the endothelial monolayer, thereby reaching the alveolar epithelium. In this connection, thrombin levels are elevated in bronchoalveolar lavage (BAL) fluid from patients with ARDS, pneumonia and in patients with ventilator-associated pneumonia (Levi M, 2003). Furthermore, recent anticoagulant strategies at microcirculatory sites of inflammation have been proved successful in patients with ALI. Together, these results illustrate the relevance of thrombin as a model to study ALI and

alveolar epithelial barrier regulation.

Thrombin is an endogenous agonist for proteinase receptor 1 (PAR-1). There is extensive evidence that in the respiratory system PARs are expressed in a variety of cell types that are relevant to inflammatory lung diseases, and that activation of these receptors might be linked to significant pathological changes (Moffatt et al., 2004b). Besides, in *in vitro* conditions, release of interleukin IL-6, IL-8, and prostaglandin E2 occurs following PAR-1 stimulation in A549 cells (Moffatt et al., 2004b;Coughlin, 1999).

PAR-1 is activated when thrombin binds to and cleaves its amino-terminal exodomain to unmask a new receptor amino terminus. This new amino terminus then serves as a tethered peptide ligand, binding intramolecularly to the body of the receptor to effect transmembrane signaling (Bogatcheva et al., 2002). Although the mechanism of

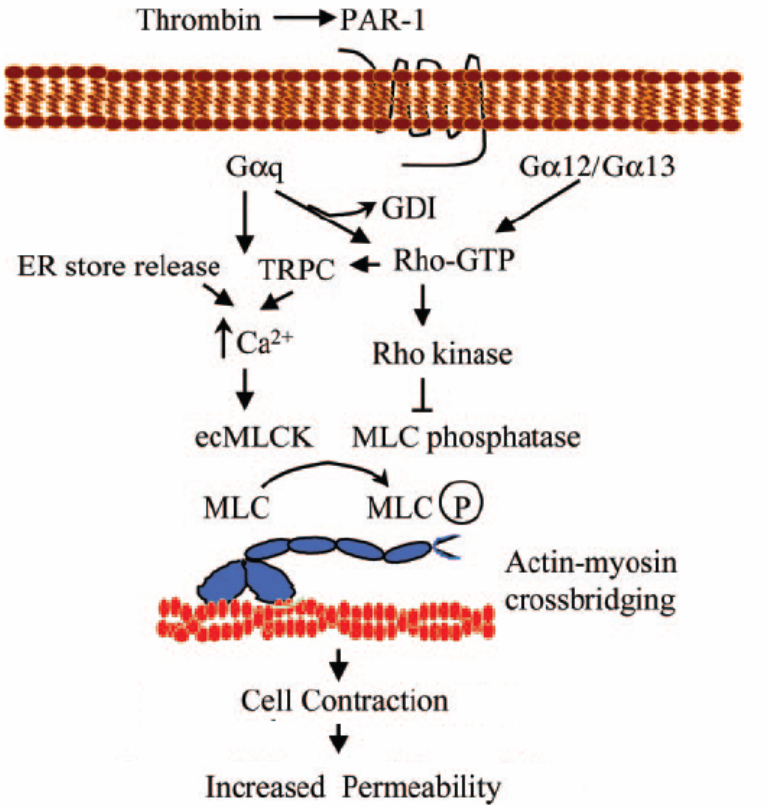

Fig. 1.5 Possible mechanisms inducing thrombin-induced cell contraction. Thrombin activates MLCK and Rho-kinase pathways, which signal MLC phosphorylation and actomyosin machinery activation, resulting in contractile force generation. Adapted from (Mehta et al., 2004).

PAR-1 activation is irreversible, a rapid trafficking behavior makes possible that an intracellular pool of thrombin receptors constantly refreshes the cell surface with naïve receptors, thereby maintaining thrombin responsiveness (Coughlin, 1999). PAR-1 interacts with multiple G protein subtypes (Fig. 1.5). The best known common signaling pathway following activation of PARs includes activation of phospholipase C via G_q protein, which produces IP_3 followed by Ca^{2+} mobilization. However, other multiple signaling pathways have also been described. Particularly, PAR-1 also interacts with $G_{12/13}$, which interacts then with Rho guanine-nucleotide exchange factors (GEFs) leading to Rho activation (Bogatcheva et al., 2002). It should be noted that thrombin activation of PAR-1 triggers two of the main pathways signaling acto-myosin contraction, namely cytosolic Ca^{2+} increase and Rho activation. Therefore, it is reasonable to think that thrombin would induce changes in the contractile state of alveolar epithelial cells. Nevertheless this hypothesis must be taken cautiously, since the extent to which PAR-1 activates each of these pathways presumably depends on the G protein and effectors repertoire expressed in each cell type (Bogatcheva et al., 2002;Trejo, 2003). In this connection, Kawkitinarong and coworkers reported increases in diphosphorylation of MLC after thrombin challenge in A549 cells (Kawkitinarong et al., 2004). This result indicates triggering of pathways signaling activation of the actomyosin machinery and possible force generation. However, direct measurements of contractile force generation after thrombin challenge are required to elucidate this hypothesis.

1.3.3 Stretch as a mechanical stimulus inducing contractile response of alveolar epithelial cells

Mechanical ventilation of the lungs is a frequently required and widely used method of patient support in clinical practice. Nevertheless, it has been shown that mechanical ventilation may be responsible for not only exacerbating pre-existing lung damage and causing multiple organ dysfunction but also for initiating injury in healthy lungs (Ricard et al., 2003). Studies performed on animals suggest that overdistension of the alveoli may be responsible for the observed lung injury (Pinhu et al., 2003;Farre et al., 2005). Nevertheless, there is little information on how alveoli deform when lung volume increases (Vlahakis and Hubmayr, 2000). In this connection, Tschumperlin and Margulies reported that alveolar walls carry little stress during normal breathing and that they simply unfold rather than undergoing deformation as the lung inflates (Fig. 1.6 left micrographs) (Tschumperlin and

Margulies, 1999). However, it has been also reported that at lung volumes approaching total lung capacity, alveolar walls indeed display distention with maximum area changes in the range 25-40% (Fig. 1.6 right micrographs) (Vlahakis and Hubmayr, 2000;Dobbs and Gutierrez, 2001). Alveolar epithelial cells sense alveolar wall distention through their attachments to neighboring cells and underlying matrix (Suki et al., 2005). Therefore, it is reasonable to think that alveolar epithelial cells will undergo similar amount of stretch as that reported for alveolar walls and basement membrane during lung inflation at high volumes (Tschumperlin and Margulies, 1999). The effect of stretch on alveolar epithelial cell contraction has been scarcely studied. Focusing on possible mechanisms regulating contractile force generation, intracellular Ca^{2+} levels have been shown to display a fast and transient increase after a single stretch application, suggesting activation of the acto-myosin machinery (Wirtz and Dobbs, 1990). Moreover, some authors have suggested that a step-wise stretch may disrupt actomyosin interactions and cytoskeletal crosslinks, reducing active force generation (Trepat et al., 2006). Therefore, direct force measurements are required to elucidate the contractile response of alveolar epithelial cells to mechanical deformation.

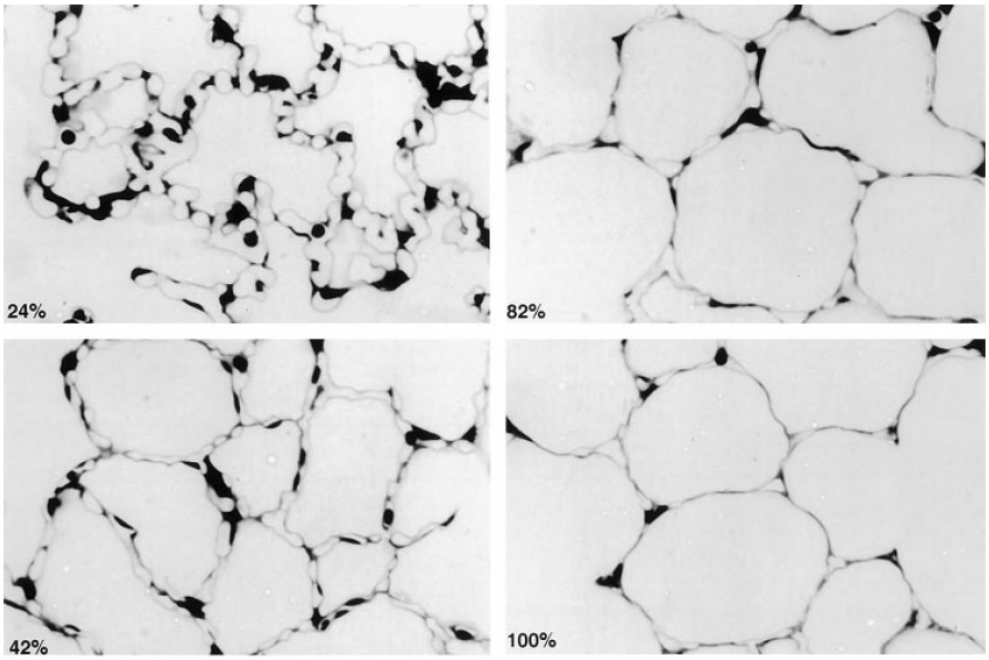

Fig. 1.6. Light micrographs of rat lungs fixed at different volumes (% of TLC). Adapted from (Tschumperlin and Margulies, 1999)

1.4 Mechanisms responsible for contractile force generation exerted by adhered cells

In eukaryotic cells, contractile force is important for the performance of a large variety of physiological functions such as cell spreading, migration, stress fibre formation, neurite outgrowth, cell contraction, and resistance to mechanical perturbations (Alberts et al., 1994). One of the main generators of contractile forces is the interaction between actin filaments and myosin. This molecular motor is estimated to exert an average maximum force of 3-5 pN during its mechanical cycle, with a net displacement during one catalytic cycle of 5.3nm and an energetic efficiency of 12-40% (Bustamante et al., 2004). Nevertheless, generation of contractile forces requires not only contraction of actin-myosin filaments but also physical linkage of these filaments to the plasma membrane and the extracellular matrix (Sylvester, 2004). In this section, the components responsible for acto-myosin contractile force generation, together with some of its regulating signalling pathways will be described.

1.4.1 Actin cytoskeleton

Actin is one of the most abundant and versatile proteins in human tissues and is widely expressed in nearly all types of eukaryotic cells. Actin assembles into a variety of structures including linear polymers in muscle, isotropic networks of filaments within the cytoskeleton, contractile stress fibers, highly organized parallel arrays of filaments in microvilli and thin protrusions of hair cells in the cochlea, as well as small oligomeric or monomeric particles and protein complexes in the cytoplasm (Bray, 2001). The actin cytoskeleton serves many cellular functions such as transmission of internal stresses, providing mechanical strength to the cell cortex and maintaining cell morphology; regulation of enzymatic activities and receptor-mediated response to external signals; spatial organization of the cytoplasm and intracellular trafficking, and cell contractility, motility and division (Bray, 2001).

Mechanical properties of actin filaments and networks

The actin globular monomer, known as G-actin, polymerizes into filamentous F-actin, which appears in electron micrographs as two right-handed helices wound around each other with a repeat distance of approximately 36 nm (Janmey, 1991). F-actin filaments *in vivo* and *in vitro* are typically some micrometers long, and measure 8 nm in diameter. The persistence length for F-actin is in the range of 3-18 μm. Both persistence length and filament length are similar, and therefore F-actin filaments can be classified as semi-flexible polymers (Janmey, 1998). Young's modulus (*E*) of one actin filament is ~2 GPa, whereas at physiologic concentrations (5-20 mg/ml) F-actin forms viscoelastic networks that exhibit a shear modulus on the order of 100–1000 Pa (Janmey, 1991;Janmey, 1998), similar to that of living cells (Alcaraz et al., 2003;Fabry et al., 2001). Finally, cross-linked F-actin networks have been shown to display strain-hardening (Gardel M.L., 2006;Xu et al., 2000).

Mechanism of actin polymerization

Actin filaments are polarized and, as a geometrical consequence, the two ends of an actin filament are structurally different and expose different portions of the actin monomer surface. In addition, the two ends have different rates of polymerization (Bray, 2001). As a consequence, the actin filament is characterized by a fast-growing (plus or barbed) end, where monomer association predominantly occurs, and a slow-growing or minus end, with predominant monomer dissociation. The polymerization of actin filaments *in vivo* requires the hydrolysis of 1 actin-bound ATP for each subunit added to the filament. Concretely, under physiological conditions, MgATP-bound G-actin is incorporated into growing filaments at the barbed end. ATP-actin is then converted into ADP-actin by slow hydrolysis as actin monomers are shifted along the filament toward the pointed ends, where filament depolymerization takes places (Disanza et al., 2005). Thus, actin assembly at steady state can be described by an ATPase cycle featuring the energetic imbalance between the fast and slow ends of filaments. Indeed, it should be noted that actin polymerization is a form of force generation. In this connection, rapid assembly of actin filaments is the principal driving force behind many forms of cell locomotion (Bray, 2001). Cells can migrate at rates up to ~0.5 μm/s (Bray, 2001) suggesting that filaments must have a net rate of elongation of ~200 monomers/s.

Actin binding proteins

In cells, the assembly and disassembly of actin filaments, and also their organisation into functional higher order networks, is regulated by a plethora of actin-binding proteins

(ABPs) which can be found in the cytoplasm of most cells. These actin regulatory proteins affect the kinetic/thermodynamic parameters of actin assembly at one or the other end of the filament in various ways (Disanza et al., 2005). Interestingly, the same basic set of actin regulatory proteins is also the convergent node of different signalling pathways emanating from extracellular stimuli (Disanza et al., 2005). Actin-binding proteins include stabilizing proteins that bind to the sides of actin filaments and prevent depolymerization (tropomyosin) and cross-linking proteins that facilitate the formation of filament bundles, branching filaments, and three-dimensional networks (Arp2/3). Other ABP include capping proteins that induce conversion of F- to G-actin (CapZ, tropomodulin), filament severing proteins that shorten the average length of filaments by cutting them into two pieces (gelsolin) and ABPs that sequester G-actin and thus maintain a pool of monomers in solution (thymosinβ4, profiling, DNaseI) (Bray, 2001;Disanza et al., 2005).

Toxins affecting the actin cytoskeleton

Actin can bind to other ligands such as drugs and toxins, which also alter its polymerization kinetics. Cytochalasin D binds to the barbed end of actin filaments and prevents further polymerization (Cooper, 1987). Latrunculin-A binds only to actin monomers and sequesters them, preventing filament polymerization (Bray, 2001). Cell pretreatment with these drugs leads to cytoskeleton disruption and significant decrease in cellular stiffness, contractility and motility (Bray, 2001;An et al., 2002;Laudadio et al., 2005;Ito et al., 2006). By contrast, Phalloidin promotes actin polymerization by strongly binding to the filaments and providing stability to them. In addition, Phalloidin shifts the equilibrium between F-actin and G-actin, lowering the critical concentration for polymerization (Cooper, 1987;Sampath and Pollard, 1991). Nevertheless, it has been found that cell migration is also inhibited by Phalloidin, showing that actin depolymerization is just as important as polymerization for cell motility (Bray, 2001).

1.4.2 Myosin

Common features of the myosin family

Myosins constitute a large superfamily of actin-dependent molecular motors. They share a common domain which interacts with actin, hydrolyzes ATP and produces movement (Sellers, 2000). Myosins are typically constructed of three functional subdomains: the head domain responsible for actin binding, ATPase activity and

generation of movement; the neck domain that usually interacts with myosin light chains or calmodulin; and a variable tail domain that commonly binds the motor cargo and determines the functional specificity of the motor (Foth et al., 2006). It is widely assumed that, throughout the myosin family, the basic mechanism of movement and force production is the same. Concretely, force is generated by mechanical cycles during which the myosin head repetitively attaches to actin, undergoes a conformational change that results in a power stroke and then detaches (Gunst and Tang, 2000). The energy required for the mechanical power is generated by the enzymatic hydrolysis of adenosine triphosphate (ATP) by the globular myosin head (Gunst and Tang, 2000;Ruegg et al., 2002).

Myosin II

Myosin II, also referred to as conventional myosin, is the major cytoskeletal protein in muscle and non-muscle cells responsible for cell contraction. Myosin II is composed of two heavy chains that form a dimmer and two pairs of light chains, the regulatory light chains and the essential light chains (Gunst and Tang, 2000). The amino-terminal portion of the heavy chains (referred to as the "head") contains the motor domain. The carboxyl-terminal part of the heavy chain consists of a coiled-coil forming sequence which constitutes the long tail. The most unique characteristic of myosin II is its ability to form filaments via the self-association of long tails (Sellers, 2000). Each myosin head is associated with an essential and a regulatory light chain, localized at the neck portion of the molecule (Gunst and Tang, 2000). Vertebrate smooth muscle and non-muscle myosin II activity is regulated by the phosphorylation of these regulatory light chains (RLCs) at two specific binding sites. These sites of phosphorylation were identified as serine 19 and threonine 18 (Ikebe et al., 1986). The phosphorylation of threonine 18 is slower than that of serine 19, whereas dephosphorylation of both the two sites has the same rate (Ikebe et al., 1986). This allows RLC to be in either the de-, mono-, or diphosphorylated state (Ikebe et al., 1986). Phosphorylation of the RLC results in a conformational change that allows actin to stimulate myosin ATPase activity, crossbridges to cycle and actin to slide past myosin (Sylvester, 2004), thus exerting contractile forces.

Within the last 10 years, several kinases involved in various signal transduction pathways have been shown to phosphorylate RLC of myosin II (Fig. 1.7). These signalling pathways are activated by both Ca^{2+}-dependent and Ca^{2+}-independent pathways. Myosin light chain kinase (MLCK) and Rho/Rho-kinase (ROK) pathways are the two major cellular targets for regulating myosin II phosphorylation and they generally operate in

parallel.

Ca^{2+}-dependent myosin light chain kinase pathway

Ca^{2+}-dependent cell contraction results from an increase in cytosolic Ca^{2+} concentration, arising from two different locations (Sylvester, 2004). On the one hand, the extracellular space, through sarcolemmal receptor-, store-, or voltage-operated Ca^{2+} channels (Sylvester, 2004). On the other hand, the sarcoplasmic reticulum, through channels known as IP_3 receptors (Fig. 1.7) (Sylvester, 2004). Cytosolic Ca^{2+} binds to calmodulin (CaM). Then the Ca^{2+}/CaM complex binds to and activates the serine/threonine protein kinase, MLCK (Fig. 1.7). The active MLCK complex catalyzes myosin II RLC phosphorylation at the two sites mentioned above, namely Ser-19 and Thr-18. MLCK is distinguished by its exquisite substrate selectivity for RLC and its ubiquitous distribution not only in smooth muscle, but also in most, if not all, nonmuscle cells (Somlyo and Somlyo, 2003). To date, all MLCK isoforms have been shown to be strictly dependent on Ca^{2+}/CaM for activation of the myosin II RLC. Finally, it has been shown that the sensitivity of MLCK to Ca^{2+} can be downregulated (Somlyo and Somlyo, 2003).

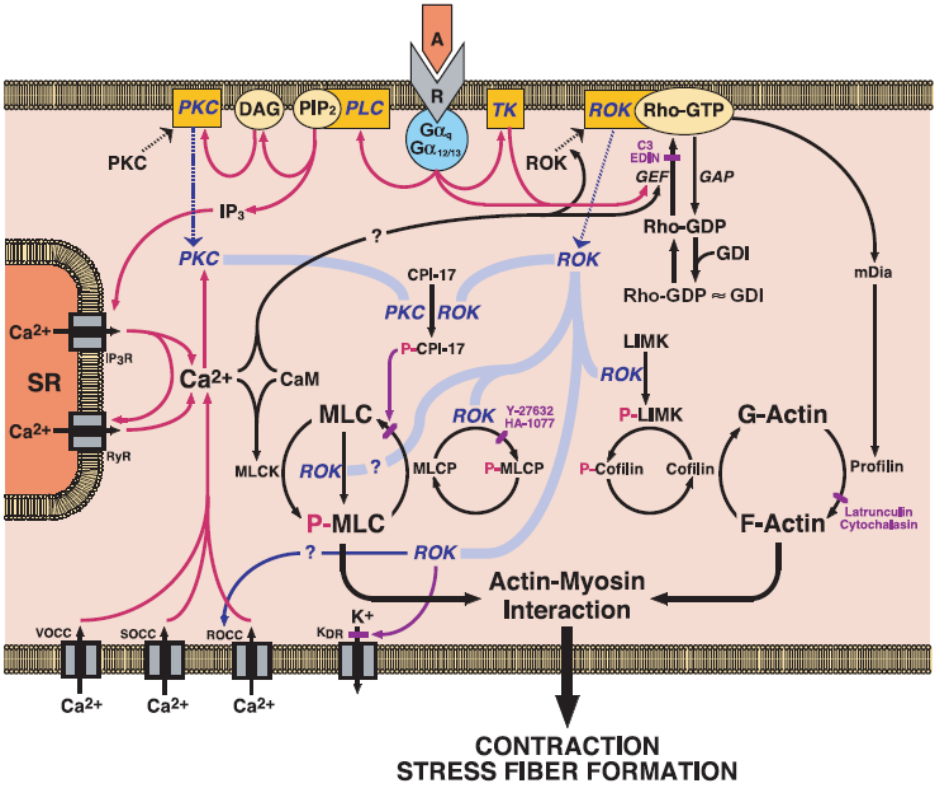

Fig. 1.7 A few of the many signaling pathways of cell contraction and some of its inhibitors. Adapted from (Sylvester, 2004).

Concretely, phosphorylation of a COOH-terminal Ser phosphorylation site reduces the affinity of MLCK for Ca^{2+}/CaM by ~10-fold. This inhibitory site can be phosphorylated by cAMP-dependent kinase, p21-activated kinase (PKA) or other kinases when Ca^{2+}/CAM is not bound to MLCK (Somlyo and Somlyo, 2003). Finally, to study the Calmodulin/MLCK signalling pathway, some inhibitors have been developed. W-5, W-7 and KT5926 are used as calmodulin inhibitors, whereas ML-7, ML-9 and Wortmannin are used as MLCK inhibitors (Katoh et al., 2001;An et al., 2002;Vouret-Craviari et al., 1998;Chrzanowska-Wodnicka and Burridge, 1996)

Rho/Rho-kinase pathway

The discovery of the Rho family of proteins initiated study of possible Ca^{2+}-independent regulation of myosin II motor activity and contraction. To date, 20 Rho proteins have been identified in humans and divided into five subfamilies based on structural and functional similarities: Rho-like, Rac-like, Cdc42-like, Rnd, and RhoBTB (Sylvester, 2004;Burridge and Doughman, 2006). Focusing to the Rho/ROK pathway, it has been shown to be the predominant mechanism responsible for Ca^{2+} sensitization, which is the process whereby contraction is stimulated when Ca^{2+} levels are held constant. Rho and the other monomeric GTPases act as molecular switches that are "on" when bound to GTP, permitting recognition and activation of target proteins, and "off" when bound to GDP (Sylvester, 2004). In the active GTP state, RhoA interacts with its effector molecules to initiate downstream responses. Activation of ROK by GTP·RhoA is the next step in the signalling pathway regulating phosphorylation of myosin II and contraction (Fig. 1.7). ROK has been proposed to regulate contraction by two distinct but functionally related processes: 1) catalyzing phosphorylation of the myosin binding subunit of myosin phosphatase at residue Thr-695, thereby inactivating myosin phosphatase and 2) direct phosphorylation of myosin II RLC at Ser-19 and Thr-18 (Emmert et al., 2004). Thus, phosphorylation of either of these substrates results in a net increase in phosphorylation of RLC, myosin II activation, and contraction.

Several bacterial toxins and exoenzymes that affect the Rho subfamily of small GTPases have been valuable to investigate the Rho/ROK signalling pathway. Concretely, the high specificity of the C3 has been used to inhibit the RhoA/ROK pathway upstream without affecting other GTPases such as Rac or Cdc42 (Garcia et al., 1999;Jacobson et al., 2004;Worth et al., 2004). Toxin B is also used to inactivate RhoA (Birukova et al., 2004;Ciano-Oliveira et al., 2005). Finally, Y-27632 or HA-1077 are extensively used as a

ROK inhibitors (Katoh et al., 2001;An et al., 2002;Ishizaki et al., 2000;Ito et al., 2006;Sah et al., 2000;Somlyo and Somlyo, 2003).

Simultaneous activation of MLC signalling pathways

Contractile agonists activate contractile responses through numerous G protein-coupled receptors. Interestingly, most $G\alpha_q$-coupled receptors activate both RhoA and phospholipase C (PLC), which induces IP_3 production and Ca^{2+} release from the sarcoplasmic/endoplasmic reticulum (Fig. 1.7) (Somlyo and Somlyo, 2003). Therefore, after a contractile challenge under physiological conditions, both Rho/ROK and MLCK pathways are often activated and act in concert. Spatial differences in the phosphorylation of RLC between the cortical and the central regions have been observed (Somlyo and Somlyo, 2003). In this connection, Katoh and coworkers reported that on human fibroblasts and endothelial cells, contraction of centrally located stress fibers depended largely on the activity of ROK, while MLCK played a major role in regulating the peripheral stress fibers (Katoh et al., 2001). These differences in spatial control by MLCK, ROK, and other kinases and myosin phosphatase may be influenced by localized sources of Ca^{2+}, inhomogeneous influx through Ca^{2+} channels, and release from the sarcoplasmic reticulum (Somlyo and Somlyo, 2003). In addition, it has also been suggested that when the two MLC signalling pathways act in concert, ROK predominantly regulates sustained contraction, whereas MLCK regulates fast duration-limited contractions (Katoh et al., 2001). Finally, in *in vitro* conditions, ROK has been shown to be more effective than MLCK in diphosphorylating RLC (Somlyo and Somlyo, 2003).

1.4.3 Focal adhesions

The adhesive interactions between a cell and its surrounding extracellular matrix (ECM) and other cells regulate its morphology, migratory properties, growth, and differentiation (Burridge and Chrzanowska-Wodnicka, 1996). Focal adhesions (FAs) are specialized sites of adhesion where the plasma membrane is held approximately 15 nm from the substrate (Bray, 2001). The major transmembrane components in FAs are integrins, a large family of transmembrane heterodimers composed of α and β subunits (Fig. 1.8). Both subunits span the membrane once and have large extracellular and short intracellular domains (Burridge and Chrzanowska-Wodnicka, 1996). Integrins bind to peptide moieties such as Arg–Gly–Asp (RGD) that are present in a number of ECM

proteins such as fibronectin, vitronectin, laminin and fibrinogen (Owen et al., 2005). As a consequence, α and β subunits combine to produce an heterodimer with a selective affinity for a particular extracellular matrix molecule (Bray, 2001). The cytoplasmic region of integrins is indirectly connected to the actin cytoskeleton via a meshwork of linking molecules such as talin, vinculin, or filamin (Fig. 1.8) (Horwitz, 1997;Critchley, 2000). These protein assemblies stabilise the focal adhesion structure, as well as relay signals from the ECM to the nucleus. Therefore, the focal adhesion is a structural unit that additionally directs the flow of information from outside the cell to the inside (Owen et al., 2005).

The area of FA is of a few μm^2 and the force per unit area has been estimated to be in the range between 1 to 10 $nN/\mu m^2$ (Balaban et al., 2001;Dembo et al., 1996;Tan et al., 2003). However, size and strength of FA depend on the mechanical properties and biochemical composition of the ECM (Choquet et al., 1997), with increasing matrix rigidity resulting in increased integrin expression (Yeung et al., 2005;Paszek et al., 2005). Interestingly, contractile forces exerted by adhered cells also increase with the rigidity of the matrix substrate and its ligand density (Saez et al., 2005;Reinhart-King et al., 2005;Paszek et al., 2005). Therefore, this suggests that FAs and cell contractility are closely correlated. It has been shown that the generation of tension, which can be either internally

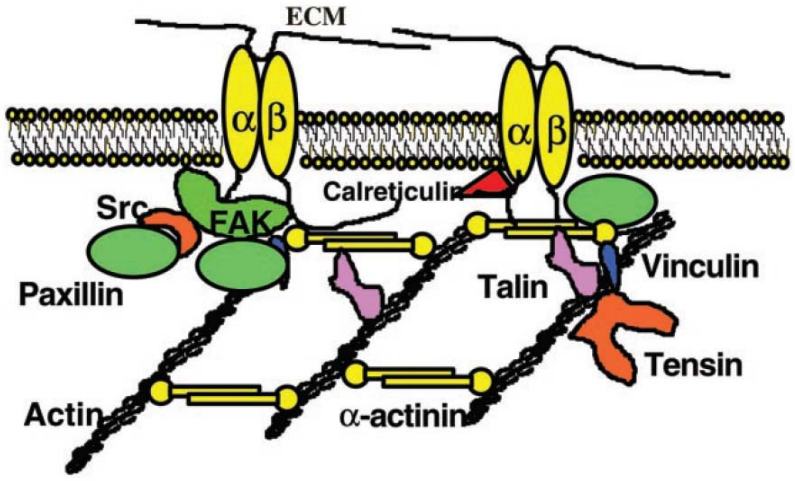

Fig. 1.8 Simplified model of a focal adhesion complex. The model depicts the types of components that are organized by integrins at points of close apposition to integrin ligands. These include kinases and dual kinase/adaptor proteins, scaffolding proteins, such as paxillin, and links to the actin cytoskeleton, such as α-actinin and vinculin. Adapted from (Sheppard, 2003).

generated by acto-myosin activity or externally applied from the outside drives the formation FAs (Galbraith et al., 2002;Burridge and Wennerberg, 2004)). Conversely, FAs disassemble when contractility is inhibited or tension is released (Burridge and Chrzanowska-Wodnicka, 1996).

1.4.4 Tensegrity, a model of cell architecture

Several models have been developed to understand how cells change their mechanical properties in response to mechanical stresses. A particularly interesting model is tensegrity, which provides a suitable paradigm to relate contractile forces, cell stiffness and cell adhesion. According to the tensegrity model, the structure of the cytoskeleton is believed to be regulated and stabilized by a preexisting tensile stress (prestress) carried by the actin filaments (Fig. 1.9). This tensional prestress is generated actively by the contractile actomyosin apparatus. In addition, passive contributions to prestress come from cytoskeleton distension through adhesions to the ECM and other cells, osmotic forces acting on the cell membrane, and forces exerted by filament polymerization (Ingber, 2003). Nevertheless, to establish a force balance, this internal prestress must be balanced by some

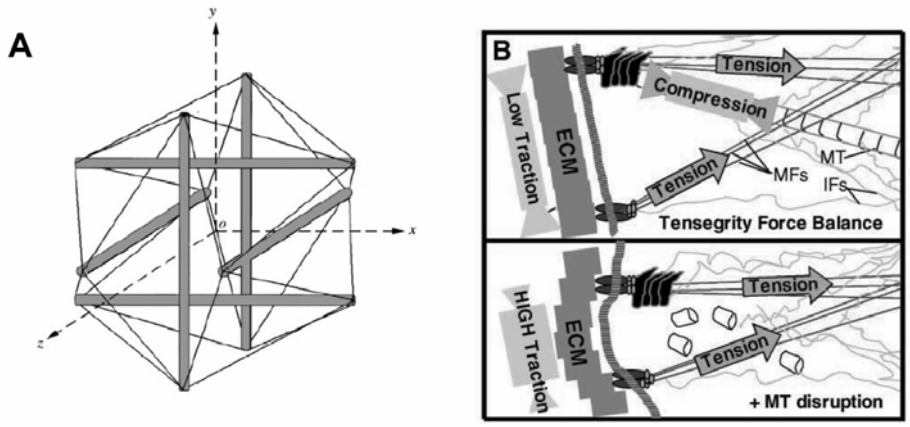

Fig. 1.9 A) Three-dimensional tensegrity structure. Tensile forces are carried by cables (thin straight lines) and resisted by struts (grey bars). In living cells, the role of the cables is thought to be played by actin microfilaments (MFs) and the role of struts by microtubules (MTs). Adapted from (Stamenovic and Coughlin, 1999). B) A schematic diagram of the force balance between tensed MFs, intermediate filaments (IFs), compressed MTs and the ECM in a region of a cellular tensegrity array. Compressive forces borne by MTs (top) are transferred to ECM through the focal adhesions when MTs are disrupted (bottom), thereby increasing substrate traction. Adapted from (Wang et al., 2002;Ingber, 2003)

sort of tension bearing elements. The tensegrity model proposes that prestress is balanced both by microtubules (MT) and the ECM through discrete points of cytoskeletal insertion onto it, namely FAs (Fig. 1.9B)(Ingber, 2003). Therefore, local regions of the ECM act like external support elements to resist cytoskeletal tensional forces. As a result, traction forces will be observed on the substrate of adhered cells correlating with sites of focal adhesion location (Fig. 1.9B) (Schwarz et al., 2003).

Tensegrity predicts a linear correlation between stiffness and cellular prestress. Accordingly, Wang and coworkers (Wang et al., 2002) experimentally found this kind of relation between cell prestress (quantified from data obtained using traction force microscopy) and cell stiffness (obtained using magnetic twisting cytometry). Finally, the tensegrity model also predicts strain-hardening when cells are subjected to external mechanical deformation (Ingber, 2003), which is a phenomenon experimentally observed in different cell types (Trepat et al., 2004;Fernandez et al., 2006).

1.5 Physical methods to probe cell contractile forces

In the past few years several methods have been developed to probe forces exerted by cells on their substrate. Two main different approaches have been used to detect cell generated forces, namely arrays of microdetectors or elastic gels. Arrays of microdetectors allow for easy computation of exerted tractions, although they require sophisticated fabrication and calibration techniques. On the other hand, transparent, non-toxic elastic gel substrates are readily prepared and their elastic properties can be easily tuned and measured. Nevertheless, since the deformations propagate through the gel, complex computation methods are required to calculate the exerted tractions from the observed deformations. All these methods will be reviewed in this section, aiming at describing their strengths and limitations.

1.5.1 Micromachined cantilevers

The first attempts to quantify cellular forces with arrays of microdetectors as force transducers used micromachined cantilevers on silicon wafers (Galbraith and Sheetz, 1997). Cells adhered and exerted forces on micrometer-sized pads at one end of a flexible cantilever, causing displacements that were detected with high precision on a light microscope (Fig. 1.10A). With this technique, strains were confined to individual cantilevers and as a consequence, traction forces could be easily calculated multiplying the spring constant of the cantilever by its displacement. The most important drawback of this technique was that the spatial resolution was highly limited by the density of cantilevers, which usually resulted in ~1 cantilever per cell. Therefore, the device could not be used to obtain a map of tractions exerted by an adherent cell, but rather to obtain time-courses of point tractions exerted by a migrating cell as it crossed the cantilever beam (Fig. 1.10E). In addition, the cantilever beams could only move in one axis, implying that the detection of force was limited to one dimension. To compute an approximate estimate of the total exerted force, the authors suggested dividing the observed displacement by the sine of the

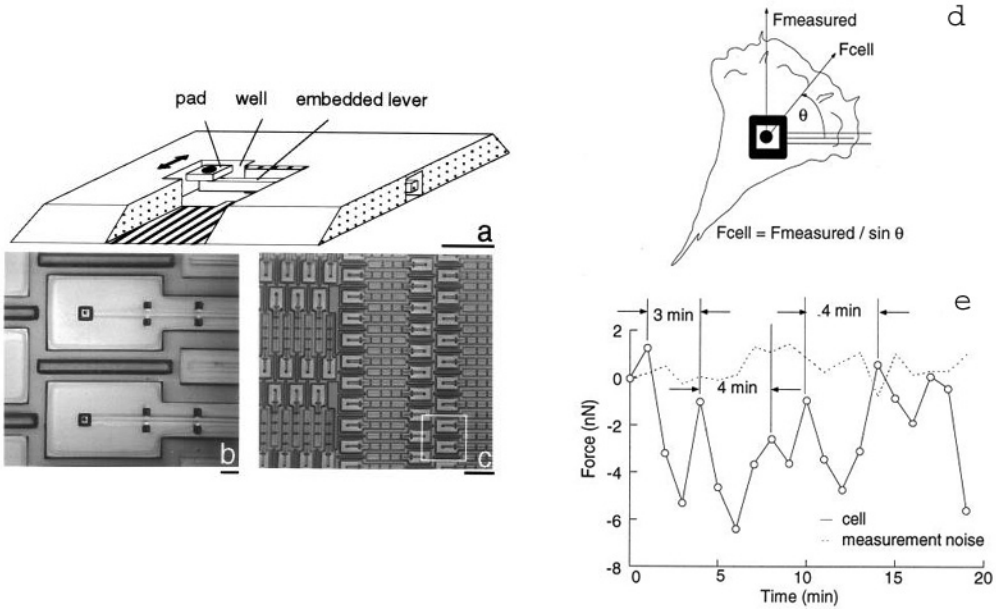

Fig. 1.10 A: A cut-away drawing showing the lever, the pad, and the well. The arrow indicates the bending direction of the lever (Bar = 10 μm.). B and C: Different magnifications of the micromachined substrate. B: Bar = 10 μm. C: Bar = 1 mm. The white square indicates the region of this photo that is presented in B. D: Force vector diagram explaining the calculation of the maximum force generated by the cell dividing the measured force by the sine of the angle the cell makes with the beam. E: A typical time-course recording showing fluctuations in force as the cell crosses the pad together with the level of noise. Adapted from (Galbraith and Sheetz, 1997).

angle that the cell made with the cantilever beam (Fig. 1.10D).

1.5.2 Microneedles

The limitations of the cantilever approach, mainly due to the one-dimensional nature of the observed displacements and the low gauge density, were overcome by using arrays of microfabricated elastomeric, microneedle-like posts (Fig. 1.11A) (Tan et al., 2003). In this method, cells attach to and deflect multiple posts, and the deflection is subsequently observed with an optical microscope (Fig. 1.11B). Similarly to the previously described method, this approach is based on detecting point-like strains confined to individual gauges. The deflection of the posts occurs independently of neighboring posts and directly reports the subcellular distribution of traction forces. In addition, the compliance of the substrate can be varied by controlling the geometry of the posts. Initial experiments used an array of posts with 9 μm spatial resolution (Tan et al., 2003). Nevertheless, the low post density affected cell adhesion and cell locomotion. In addition, cells did also attach to the base substrate beneath the flexible post, resulting in force underestimation (Fig. 1.11C) (Tan et al., 2003). The technique has been refined to provide higher spatial resolution of the observed traction fields, reaching ~3 μm spatial resolution and 1nN force resolution (du Roure et al., 2005). Nevertheless, technical limitations arise as the diameter of the posts is reduced and its aspect ratio is increased (Roca-Cusachs et al., 2005). It has been reported that posts with small diameter and low Young's modulus will collapse due to ground

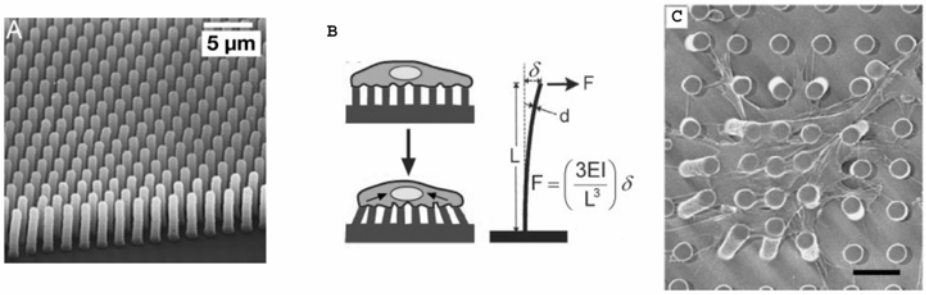

Fig. 1.11 A: Scanning electron micrograph of a high density array of microfabricated posts. B: Schematic drawing of the method used to compute traction forces. With the appropriate surface density of vertical posts, a cell should spread across multiple posts as depicted. Under the proper geometric constraints of post height and width, cells exerting traction forces (*F*) would deflect the elastomeric posts by a certain amount of displacement (*δ*). C: Scanning electron micrograph of a smooth muscle cell attached to low density array of posts (bar = 10 μm). It can be observed that the cell attaches at multiple points along the posts as well as the base of the substrate. (Tan et al., 2003) and (du Roure et al., 2005).

adhesion. Therefore, this drawback limits the applicability of the technique to measure very small tractions with high spatial resolution.

1.5.3 Wrinkling of silicone films

The basic idea of using an elastic substrate to study the forces produced by single cells was originally conceived by Harris and coworkers (Harris et al., 1980; Harris, 1988). Flexible substrates were produced by inducing polymerization of a very thin film of silicone on the surface of liquid silicone. Compressive forces exerted by adherent cells induced buckling of the film and the consequent wrinkle field provided a highly visible semiquantitative readout of the exerted tractions (Fig. 1.12). This method was thought to be sensitive to nano-Newton forces (Beningo and Wang, 2002), but it could not provide a simple way to convert the pattern of wrinkles into a map of traction forces. Moreover, the wrinkles developed very slowly and were nonlinear and chaotic. These characteristics severely limited the spatial and temporal resolution of the technique, in addition to providing only a crude estimate of cell tractions.

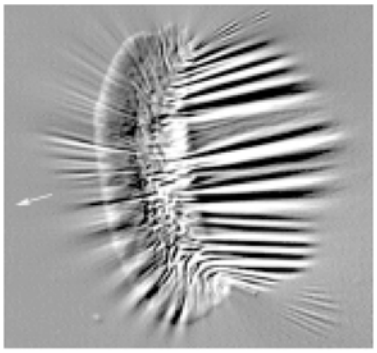

Fig. 1.12 Motile fish keratocyte on a wrinkling silicone substratum. Arrow indicates direction of migration. (Beningo and Wang, 2002)

1.5.4 Contraction of collagen gels measured by gel area reduction or by force transducers.

The basic idea of using elastic gel substrates to probe cell contraction was extended by the introduction of collagen I gels. Interestingly, collagen is a physiologically suitable extracellular matrix that enables cell culture on the top or inside the gel substrate (Umino et al., 2000). The simplest approach to probe cell contraction consists in culturing the cells on collagen gels floating on culture medium (Umino et al., 2000;Fang et al., 2004). Since the

collagen gel is not attached to the bottom of the culture well, cell contraction induces reduction of the gel area, which is then measured with an image analyzer device. This approach does not provide an estimate of the amount of force exerted by the cell and has been solely used to qualitatively assess cell-mediated gel contraction or relaxation after challenge with different contractile agonists or antagonists (Fig. 1.13).

Quantification of the force exerted by cells cultured on collagen gels is accomplished by attaching the cell-cultured collagen gels to force transducers (Bodmer et al., 1997). The collagen gel is polymerized between two pairs of perpendicular-placed polyethylene bars which are then connected to two force transducers, providing a quantitative estimate of the net aggregate force (Fig. 1.14A). In addition, the use of force transducers allows higher time resolution than that reported in measurements of gel area changes (Fig. 1.14B). Nevertheless, cultured adherent cells exert low levels of tension and as a consequence signal acquisition is very susceptible to interference from background electrical and mechanical noise (Fig. 1.14C). This technique has been successfully used to quantitatively measure the time-course of the contraction induced by contractile agonists on a cell monolayer (Moy et al., 1996;Moy et al., 2002).

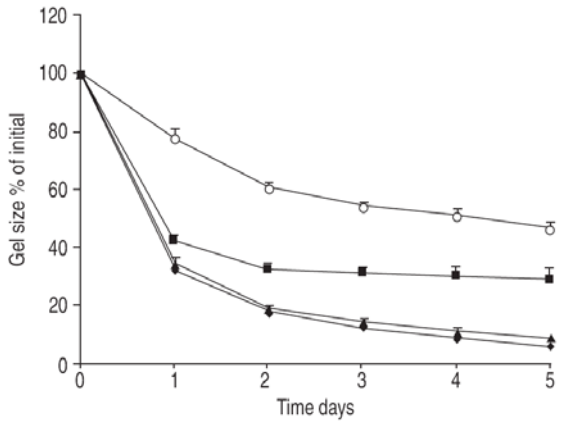

Fig. 1.13 Effect of different doses of a contractile agonist on the collagen gel contraction mediated by human fetal lung fibroblasts. Each symbol corresponds to different concentrations of contractile agonist. Data are presented as relative values of initial gel size. Adapted from (Fang et al., 2004).

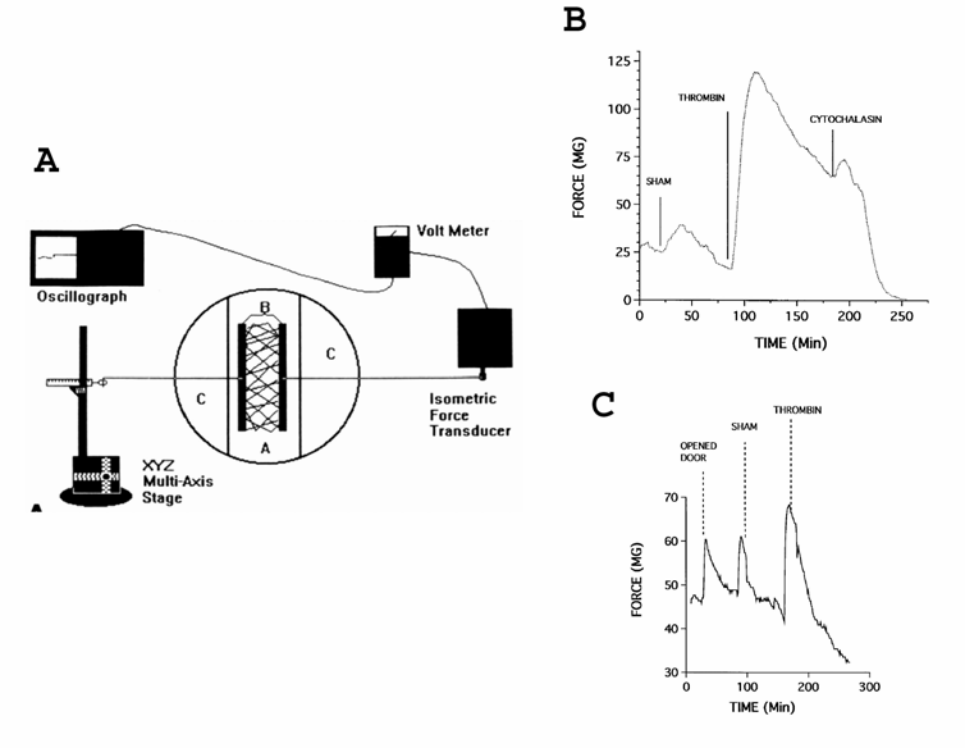

Fig. 1.14 A: A schematic representation of the isometric force monitoring apparatus containing only one force transducer. One of the holders is attached to a multiaxis stage manipulator, and the other is attached to an isometric force transducer. Force is monitored with a voltimeter and recorded with an oscillograph. B: The effect of the contractile agonist Thrombin and the cytoskeleton depolymerizer Cytochalasin D on the isometric tension exerted by cultured HUVEC. C: Example of the effect of noise (opening the incubator door) on the electric measurement of gel contraction Adapted from (Goeckeler and Wysolmerski, 1995;Bodmer et al., 1997).

It should be noted that this method (measured either by changes in area or by force transducers) provides only an estimate of the total amount of force exerted by an undetermined number of cells. Therefore, this technique does not allow estimation of the amount, distribution or direction of traction forces exerted by a single cell

1.5.5 Traction microscopy

The applicability of elastic gel substrates to measure traction forces was greatly enhanced by embedding fluorescent microbeads into them (Fig. 1.15). With this procedure, local deformations of the gel induced by a single adhered cell can be detected simply by measuring the displacements of the fluorescent beads. Traction microscopy enables

quantification of the amount and distribution of forces exerted by a cell. In order to measure the total amount of force generated by a cell, exerted forces must be balanced solely by the gel substrate. Therefore, traction microscopy must be performed on single cells lacking contacts with neighboring cells. Soon after this approach was first proposed, collagen-coated polyacrylamide gels became the standard elastic substrates used in traction microscopy experiments, because they are easy to prepare, elastic and allow better image acquisition with an optical microscope than silicone or collagen gels. Collagen coating prevents direct contact of the cells with the polyacrylamide substrate, constituting a suitable ECM for the adhered cells. Moreover, collagen-coated polyacrylamide gels have been shown to display no cytotoxicity (Damljanovic et al., 2005). The added benefit of polyacrylamide is that its stiffness can be readily adjusted by controlled variations of the monomer and cross-linker concentrations (Yeung et al., 2005). Thus, regardless of the stresses produced by a particular cell type, controlled linear deformations with a detectable magnitude can always be achieved just selecting the suitable gel stiffness.

Deformation of the gel due to the adhered cell is determined by comparing images of the cell-deformed substrate with a null-force image, which must be recorded after removing the cell by physical or chemical means. This technique allows dynamic stimulation of the studied cell and time-course recording of its contractile evolution for long periods of time. Nevertheless, it should be noted that the experimental protocol must

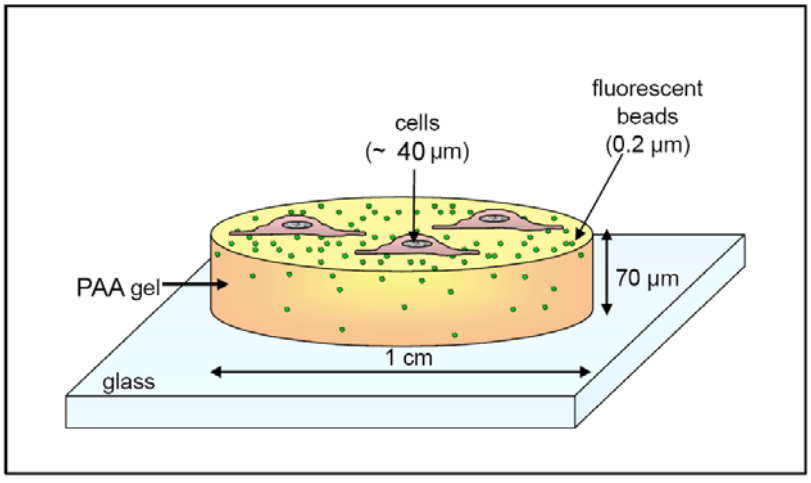

Fig. 1.15 Traction microscopy experimental setup. The cells are plated on a flexible polyacrilamide gel disc with embedded fluorescent microbeads. Cellular traction forces induce deformation of the gel and hence displacement of the microbeads. These displacements are used to compute the traction.

end by imaging the cell-free gel to allow for computation of the absolute values of traction forces. Computation of substrate deformation from a pair of fluorescence images is carried out using optical flow or correlation-based algorithms (Marganski et al., 2003;Tolic-Norrelykke et al., 2002). Using a high density of fluorescent microbeads per imaged field and interpolation algorithms, maps of gel deformation can be obtained with ~1 μm spatial resolution and 10–100 nm precision (Fig. 1.16 left) (Marganski et al., 2003;Tolic-Norrelykke et al., 2002). Once the displacement map is obtained, the traction field is computed using information of the gel properties, such as the Young's modulus or the Poisson ratio of the gel. Interestingly, knowledge of the traction field allows quantification of the amount, distribution and direction of traction forces exerted by the adherent cell (Fig. 1.16 right). It should be noted that strains exerted on uniformly flexible substrates propagate across it and fall of as a function of the distance from the source of stress (Butler et al., 2002). Consequently, conversion of maps of substrate deformation into maps of traction forces requires intensive large scale matrix computations (Dembo and Wang, 1999). This issue was solved by Butler and coworkers (Butler et al., 2002), who proposed computation of traction forces on the Fourier domain. This approach enables fast, simple and exact computation of the traction field from the previously obtained displacement field, maintaining ~1 μm spatial resolution.

Since Dembo and Wang published the mathematical fundaments to compute traction forces from observed gel displacements in 1999, a considerable number of published studies have used this technique, usually referred as traction microscopy (TM). TM has been used to report distribution of traction forces of migrating cells (Dembo and Wang, 1999), contraction of muscular and non-muscular cells after chemical, electrical or

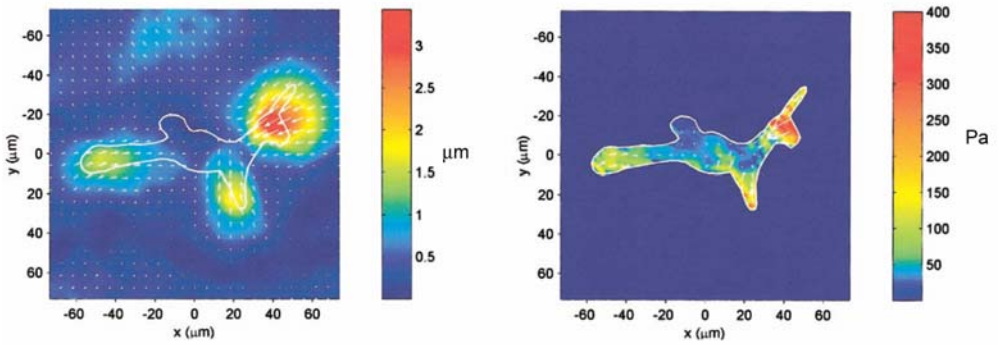

Fig. 1.16. Example of a displacement field (left) exerted by an HASM cell cultured on a polyacrilamide gel and the corresponding traction field (right). Adapted from (Butler et al., 2002).

mechanical challenge (An et al., 2002;Hu et al., 2003;Wang et al., 2002), and dependence of cell contractility on the rigidity of the substrate or the ligand density of the extracellular matrix where the cell is adhered (Yeung et al., 2005;Reinhart-King et al., 2005;Paszek et al., 2005). In this thesis, TM will be used to measure contraction of alveolar epithelial cells induced by biochemical (thrombin) or mechanical (stretch) stimuli.